frontiers | Frontiers in Materials

TYPE Original Research
PUBLISHED 04 April 2024
DOI 10.3389/fmats.2024.1371351

OPEN ACCESS

EDITED BY
Luca Valentini,
University of Perugia, Italy

REVIEWED BY
Enze Zhou,
Northeastern University, China
Hongwei Liu,
Sun Yat-sen University, China
Margherita Izzi,
University of Bari Aldo Moro, Italy

*CORRESPONDENCE
Dawei Zhang,
dzhang@ustb.edu.cn

RECEIVED 16 January 2024
ACCEPTED 21 March 2024
PUBLISHED 04 April 2024

CITATION
Yang J, Ran Y, Zhao J, Xing T, Hao X and Zhang D (2024), D-amino acid/gentamicin loaded zwitterionic hydrogel coatings with optimized mechanical stability and biofilm inhibition capabilities.
Front. Mater. 11:1371351.
doi: 10.3389/fmats.2024.1371351

D-amino acid/gentamicin loaded zwitterionic hydrogel coatings with optimized mechanical stability and biofilm inhibition capabilities

Jingzhi Yang[1,2], Yami Ran[1,2,3], Junsen Zhao[1,2], Taiwei Xing[1,2], Xiangping Hao[2,4] and Dawei Zhang[1,2,3]*

[1]Beijing Advanced Innovation Center for Materials Genome Engineering, Institute for Advanced Materials and Technology, University of Science and Technology Beijing, Beijing, China, [2]National Materials Corrosion and Protection Data Center, University of Science and Technology Beijing, Beijing, China, [3]BRI Southeast Asia Network for Corrosion and Protection, Shunde Graduate School of University of Science and Technology Beijing, Foshan, China, [4]School of Materials Science and Engineering, University of Science and Technology Beijing, Beijing, China

Biofilms associated bacterial infections on material surfaces have become a tremendous biomedical challenge. Developing antimicrobial coatings on biomaterial surfaces and endowing them with decent mechanical stability and biofilm inhibition capabilities is an efficient way to resist bacterial attachment and biofilm formation. Herein, we integrated 2-hydroxyethyl methacrylate (HEMA) and D-amino acid mixtures based antibiofilm combinations with sulfobetaine methacrylate (SBMA) hydrogel coatings. The obtained hydrogel coatings demonstrated high stability in various transport and service environments. The proper incorporation of the HEMA achieves only ~3% weight loss of SBMA hydrogel coatings after swelling, flushing and abrasion damages. In addition, both biofilm formation inhibiting D-amino acid mixtures and bacteria-killing gentamicin components were loaded in the coatings. The synergistic action of these two components was able to significantly reduce the bacterial numbers with up to 2.3 log reduction. The bacteria exposed to D-amino acid mixtures was difficult to form biofilm, which was more susceptive to the harm of gentamicin. This work provides an effective paradigm to integrate mechanically stable SBMA-HEMA hydrogel with natural D-amino acid mixtures based antibiofilm agents to generate biomedical surfaces to combat biofilms associated bacterial infections.

KEYWORDS

zwitterion, D-amino acids, antibiofilm coatings, drug cocktails, mechanical stability

Introduction

Owing to the desired mechanical strength, corrosion resistance, biocompatibility and relatively low cost, 316 L stainless steels are widely used in clinical practice for internal medicine diagnosis and surgical implantation (Qian et al., 2019; Yang et al., 2021). Implantable biomedical materials are initially provided to cure diseases and save lives for patients, but their surfaces are more susceptible to bacterial colonization and provide an ideal site for mature biofilm formation (Huang et al., 2020a). As a self-produced matrix

of extracellular polymeric substances (EPS), biofilm is the main living form for attached bacteria (Bjarnsholt et al., 2013; Flemming, et al., 2016). The biofilms can be seen as a fortress, bacteria encapsulated in them tend to resist the harm of the immune response and antimicrobial agents (Karatan and Watrick, 2009; Lopez et al., 2009). It is worth noting that, the presence of biofilm allows dormant bacteria to escape and survive from the sub-inhibitory concentrations of antibiotics, resulting in the transfer of drug-resistant genes to their descendants (Brauner et al., 2016). Bacterial infections become extremely difficult to treat because of the performance of biofilm. Thus, it is urgently needed to endow implantable biomedical materials with the antibiofilm capability (Busscher et al., 2012; Koo et al., 2017).

Amino acids are well-known essential nutrients for living organisms. Compared to the more widely distributed L-amino acids, their D-enantiomers are mainly discovered in the peptidoglycans of the bacterial cell membrane, and play a vital role in the maintenance of bacterial internal osmotic pressure (Conrad et al., 1974; Caparros et al., 1992). Recently, exogenous D-amino acids have been demonstrated to inhibit the formation of bacterial biofilms via the incorporation into the peptidoglycan of bacterial cells (Pedro et al., 2003; Xu and Liu, 2011; Tong et al., 2014). For example, Kolodkin-Gal *et al.* confirmed the biofilm formation inhibition performance of D-tyrosine (D-Tyr). D-Tyr was found to be incorporated into bacterial membranes via ^{14}C-D-tyrosine tracer method (Kolodkin-Gal et al., 2010). Subsequently, some researchers indicated the significantly improved antibiofilm performance of D-amino acid mixtures compared to using D-amino acids alone. Hochbaum *et al.* first showed that D-tyr, D-proline (D-Pro) and D-phenylalanine (D-Phe) mixtures exhibited a more potent ability in inhibiting the biofilm formation of *Staphylococcus aureus* than any amino acids alone (Hochbaum et al., 2011). Moreover, antimicrobial strategies to treat recalcitrant biofilm from pathogens rely heavily on drug combinations in the cases where single agents are ineffective. D-amino acids are demonstrated potential enhancers for some common clinical antibiotics such as amikacin (She et al., 2015), ciprofloxacin (Warraich et al., 2020) and so on (Sanchez et al., 2014). Therefore, D-amino acids/antibiotics combinations are promising to act synergistically to endow implantable materials with high-efficiency antibiofilm and antimicrobial effects to overcome biofilms associated bacterial infections.

Inspired by natural cell membranes, benefiting from high hydrophilicity and low cytotoxicity, zwitterionic hydrogels have attracted a lot of attention, and exhibit a powerful repulsive force against biofouling while possessing good drug-loading capacity (Wegst et al., 2015; Cao et al., 2016; Li et al., 2018; Feng et al., 2020). However, the anchoring of zwitterionic hydrogels on the material surface is limited by their unsatisfying mechanical stability (Kardela et al., 2019). Researchers focused on introducing adhesion motifs to improve the stability of zwitterionic hydrogel coatings (Gong et al., 2012; Huang et al., 2017a). For example, Dizon *et al.* synthesized a zwitterionic copolymer composed of the antifouling unit sulfobetaine acrylamide (SBAA) and the biomimetic anchoring group dopamine methacrylamide (DMA). This copolymer exhibits stable antifouling performance against *Escherichia coli* on various material surfaces (Dizon et al., 2018). Due to the lack of necessary antifouling or high hydrophilicity behavior, the copolymeric adhesion motifs would inevitably compromise the intrinsic antifouling and drug-loading capacity of the zwitterionic hydrogel. As another well-proved antifouling material (Tan et al., 2008; Sin et al., 2014), 2-hydroxyethyl methacrylate (HEMA) polymers showed good elastic properties (Kim et al., 2005). The introduction of HEMA was expected to increase the toughness of zwitterionic hydrogels, thereby improving the mechanical stability of zwitterionic hydrogel coatings (Zeng et al., 2014). In the meanwhile, fine-designed zwitterion-HEMA copolymers would have excellent drug-loading capacity resulting from their high hydrophilicity and swelling property, providing a desirable reservoir to store adequate D-amino acid mixtures based antibiofilm combinations.

In this work, antifouling zwitterionic hydrogels comprising sulfobetaine methacrylate (SBMA) monomers and mechanically stable-promoting segments HEMA were prepared and immobilized onto 316 L stainless steel. Subsequently, the SBMA-HEMA hydrogel coating matrix was loaded with D-amino acid mixture/gentamicin combinations via a feasible solution immersion manner. The mechanical stability of as prepared hydrogel coatings was systematically investigated via swelling, flow and tape-peeling tests, respectively. The UV-Vis spectra were used to monitor the time-dependent release behaviors of the D-amino acid mixture and gentamicin. The antibiofilm and antimicrobial performance against *Pseudomonas aeruginosa* of the hydrogel coatings was evaluated via spread plate method, fluorescence microscopy and crystal violet (CV) staining.

Experimental section

Materials

The 316 L stainless steel substrates were cut into the size of 10 × 10 × 3 mm and continuously ground by 400, 800, and 1200 grit abrasive papers before use. All D-amino acids used in this work, gentamicin sulfate, poly (ethyleneglycol) dimethacrylate (PEGDMA), poly (ethylene glycol) methacrylate (PEGMA), o-phthalaldehyde, β-mercaptoethanol and sodium borate solution were purchased from Aladdin Industrial Corporation. Sulfobetaine methacrylate (SBMA), 2-hydroxyethyl methacrylate (HEMA) and 2-hydroxy-4′-(2-hydroxyethoxy)-2-methylpropiophenone (photoinitiator 2959) were purchased from Sigma-Aldrich. All reagents were used without further purification. The *P. aeruginosa* (ATCC15692) strains were acquired from China General Microbiological Culture Collection Center, Beijing, China.

Preparation of D-amino acid/gentamicin loaded hydrogel coatings

Generally speaking, the final properties of the hydrogel coatings were regulated by various parameters, such as monomer content, types of crosslinker, crosslinking degree and so on (Dulong et al., 2004; Kim et al., 2009; Dizon et al., 2018). In our previous work, we optimized these three parameters for two SBMA-HEMA hydrogel coatings with different monomer ratios (1:1 and 3:1) and pure HEMA hydrogel coatings towards improving their mechanical stability and drug-loading capacity (Yang et al., 2023a).

TABLE 1 Feeding amount for preparation of hydrogel coatings in this work.

Samples	Monomer ratios	Monomer content (%)	Crosslinker content and molecular weight
$PS50H50_{op}$	SBMA:HEMA = 1:1	40	10%,200
$PS75H25_{op}$	SBMA:HEMA = 3:1	40	5%,600
$PEGMA_{op}$	PEGMA (Mn~475)	40	10%,1000
$PHEMA_{op}$	HEMA	40	25%,600

In addition, pure PEGMA hydrogel coatings were also involved in this study. The detailed formula of these four hydrogel coatings was exhibited in Table 1. The SBMA-HEMA hydrogel coatings with monomer ratios 1:1, 3:1, the pure PEGMA hydrogel coatings and the pure HEMA hydrogel coatings were hereinafter referred to as $PS50H50_{op}$, $PS75H25_{op}$, $PEGMA_{op}$ and $PHEMA_{op}$ coatings. $PS25H75_{op}$ coatings were uninvolved in this study because more HEMA components would lead to the sacrifice of drug loading capabilities of the coating. The hydrogel coatings were prepared by UV induced free radical polymerization on the clean 316 L stainless steel surfaces. Taking the $PS50H50_{op}$ coating as an example, the monomers SBMA (2.0 g), HEMA (2.0 g), the crosslinker PEGDMA (Mn~200, 0.4 g), and the photoinitiator 2959 (0.16 g, 4% of the total monomer mass) were added into a dry glass sample bottle containing 10 mL deionized water. The mixtures were sonicated for 5 min for complete dissolution and homogeneity. 70 μL mixture solution was drop-coated onto the preprocessed 316 L stainless steel surface and polymerized under UV light for 3 min (365 nm, 60 mW/cm^2). The as-prepared hydrogel coatings were immersed into the deionized water for 3 days to fully remove the unreacted chemicals. Subsequent, 75 μmol D-Tyr, 75 μmol D-tryptophan (D-Try), 300 μmol D-leucine (D-Leu), 50 μmol D-Phe and 20 mg gentamicin sulfate were dissolved completely in 20 mL of deionized water to prepare the D-amino acid mixtures (hereinafter referred to as D-mix) and gentamicin drug combination solution. This unique solution was formulated in our previous work (Yang et al., 2023b) and demonstrated excellent antibiofilm and antimicrobial properties. The hydrogel coatings were immersed in the solution overnight to achieve the purpose of D-mix and gentamicin loading.

Composition of hydrogel coatings

The as-prepared hydrogel coatings were equilibrated at room temperature for two hours before the composition characterization. The hydrogels were scraped off with a scalpel and ground into the powder. Subsequently, the hydrogel powder was thoroughly mixed with spectroscopic grade potassium bromide (KBr) powder in an agate mortar. The powder mixture was pressed into transparent thin slices using a mini-pellet press. Fourier transform infrared spectroscopy (FTIR) was utilized (Thermo Fisher Scientific, United States of America) to analyze the composition of the hydrogel coatings. The wavenumber range was set to 500–4000 cm^{-1} for the FTIR characterization.

Mechanical stability tests

The mechanical stability of hydrogel coatings was simultaneously evaluated by swelling, flow and abrasion tests. The swelling tests were performed according to the method in Section 2.4 for 72 h. In the flow test, the hydrogel coatings were placed into the bottom of a closed container for 72 h with a constant 500 mL min^{-1} flow rate controlled by a peristaltic pump (FlexPump, France) (Yang et al., 2023a). The stability of the hydrogel coatings was also investigated by the tape-peeling abrasion test according to the method reported in ASTM D3359-09 (Pacaphol and Aht-Ong, 2017). The 3M tapes (CT-18, 600#) were pressed firmly on the hydrogel coating surface with a force of 50 N and subsequently peeled off at an angle of 45°. The above process was repeated for 10 cycles for each hydrogel coating. The weight loss (WL) of the coatings was calculated by the following Eq. 1.

$$WL = (WL_0 - WL_1)/WL_0 \times 100\% \quad (1)$$

in which WL_0 and WL_1 were the weights of hydrogel coatings before and after the tests. Three parallel samples were measured for each coating, and the average value of these measurements was taken as the final result.

Swelling property tests

The as-prepared hydrogel coatings were weighted after being equilibrated at room temperature for two hours. The coatings were immersed in deionized water for 0.5 h, 1 h, 2 h, 4 h, and 8 h, respectively. Subsequently, the coatings were taken out from the deionized water and gently wiped with the filter paper to remove the remaining moisture on their surface. The weight of these hydrogel coatings was measured at different time intervals. The equilibrium water content (EWC) of hydrogel coatings after immersing for different times was calculated by the following Eq. 2.

$$EWC = (W_t - W_0)/W_0 \times 100\% \quad (2)$$

in which W_t and W_0 were the weight of hydrogel coatings at different time points and the weight of initial coatings. Three parallel samples were measured for each coating, and the average value of these measurements was taken as the final result.

Release of D-mix and gentamicin from hydrogel coatings

The absorbance curves of different concentrations (40 ppm, 20 ppm, 10 ppm, 5 ppm, 2 ppm and 1 ppm) of D-mix solution were measured via UV-Vis spectra (Hitachi, Japan). The results were fitted to plot the standard UV-Vis curves of D-mix. To characterize the release behaviors of D-mix, the water-swollen equilibrium hydrogel coating in the D-mix/gentamicin solution was put into a glass container containing 50 mL of deionized water. For each time interval (0.5 h, 1 h, 2 h, 4 h, 8 h, 24 h), 3 mL of solutions in the glass container were sampled to measure the UV-Vis absorption curve between 200 and 400 nm wavelength. After the measurement, the solutions were reintroduced into the container.

Owing to the absence of UV-Vis absorption curve of gentamicin, the release behaviors were measured according to the literature (Sampath and Robinson, 1990). Briefly, 2.5 g o-phthalaldehyde, 62.5 mL of methanol, and 3 mL of 2-mercaptoethanol were added to 560 mL of sodium borate solution at pH 8 to prepare the o-phthaldialdehyde reagent. The reagent was stored in the dark for 24 h before use. Then, different concentrations (40 ppm, 20 ppm, 10 ppm, 5 ppm, 2 ppm and 1 ppm) of gentamicin solution were mixed respectively with isopropanol and o-phthaldialdehyde reagent in a volume ratio of 1:1:1. UV-Vis absorption curve of the mixed solution was measured and the standard curves of gentamicin were plotted. To characterize the release behaviors of gentamicin, 1 mL of solutions in the glass container were sampled and mixed with 1 mL isopropanol and 1 mL o-phthaldialdehyde reagent in the dark for 1 h before the UV-Vis absorption curve measuring. The wavelength was set to 200–400 nm.

Antimicrobial activity tests

The antimicrobial activity of hydrogel coatings against *P. aeruginosa* strains was investigated by the spread plate method and fluorescence microscope method. *P. aeruginosa* cells were cultivated in a shaking Luria-Bertani (LB) fluid medium at 37°C for 18 h before use. The hydrogel coatings were co-cultured with 2 mL bacterial suspension (10^6 CFU mL^{-1}) for 24 h. After the incubation, the samples were removed from the bacterial suspensions and gently rinsed with sterile water to remove the non-adherent bacteria. For the spread plate method, the samples were immediately transferred to sterile tubes containing 3 mL LB. The attached bacteria on the sample surfaces were collected in the tubes via strong vortex oscillations. The bacterial suspensions in tubes were diluted and 50 μL of them was spread onto LB agar plates. The plates were incubated at 37°C for 24 h and the antimicrobial efficiency (AE) of the coatings was calculated by the following Eq. 3.

$$AE = \left(1 - S_{exp}/S_{con}\right) \times 100\% \quad (3)$$

in which S_{exp} and S_{con} were the CFU numbers of the experiment samples and the control samples (bare steels). Two parallel samples were measured for each coating, and three parallel plate experiments were performed for each sample. The average value of these measurements was taken as the final result.

For the fluorescence microscope method, the samples were immediately transferred into 24-well culture plates containing 20 μL STYO-9 and propidium iodide (PI) dye. The adhered bacteria on the sample surfaces were stained for 20 min in the dark and observed via confocal laser scanning microscopy (CLSM) (Model C2 Plus, Nikon, Japan). Under the field of view of CLSM, live and dead bacteria were indicated green fluorescence (488 nm) and red fluorescence (559 nm), respectively.

Antibiofilm activity tests

The antibiofilm activity of hydrogel coatings was investigated by CV staining assay in 96-well culture plates according to the literature (Sanchez et al., 2014; Huang et al., 2020b). Typically, 100 μL bacterial suspension (10^6 CFU mL^{-1}) was pre-loaded into each well of the plates, and a high-concentration D-mix solution was added to obtain a final concentration of 40 ppm for D-mix. After 48 h of incubation, LB fluid media containing high-concentration gentamicin was added into each well to make a final concentration of 13 ppm for gentamicin. The 96-well culture plates were incubated for another 24 h at 37°C. Subsequently, the plates were rinsed with sterile distilled water, and the adhered cells were stained with 100 μL of 0.1% crystal violet. For the semi-quantitative analysis of biofilm growth, the bound dye was released by 200 μL 4% (w/v) sodium dodecyl sulfate (SDS) and measured via a microplate reader at 570 nm. Antibiofilm efficiency was calculated by the following Eq. 4:

$$\text{Anti} - \text{biofilm efficiency} = \left(OD_c - OD_e\right)/OD_c \times 100\% \quad (4)$$

in which OD_c and OD_e were the OD values of the blank control samples and experimental samples, respectively. The final concentrations (40 ppm for D-mix and 13 ppm for gentamicin) used in the tests were determined by the release behaviors of D-mix and gentamicin from hydrogel coatings.

Results and Discussion

Preparation of the hydrogel coatings

Figure 1 showed the schematic diagram of the hydrogels composed of different ratios of SBMA, HEMA and PEGMA segments. The chemical composition of the obtained hydrogel coatings was investigated and characterized by FTIR (Figure 2). The $PHEMA_{op}$ hydrogel coating exhibited multiple characteristic absorption peaks, among which the broad peak at 3,400 cm^{-1} corresponds to the stretching vibration of O-H in HEMA (Tan et al., 2008). The deformation vibration at 1406 cm^{-1} and the torsional vibration at 815 cm^{-1} of CH_2 = CH are relatively weak. This result indicated that the C=C double bonds of acrylate were consumed in the photopolymerization reaction, resulting in the generation of $PHEMA_{op}$ hydrogels (Lin et al., 2006). The peaks at 1350 cm^{-1} in the FTIR spectrum of $PEGDA_{op}$ hydrogel coating were related to the stretching vibration of CH_2, while the absorption peak at 1096 cm^{-1} corresponded to the stretching vibration of C-O-C in the coatings (Xing et al., 2011). As for $PS50H50_{op}$ and $PS75H25_{op}$ hydrogel coatings, the broad peak at 3,400 cm^{-1} (O-H) also appeared in the spectrum. Moreover, the existing peaks at around 1148 cm^{-1}

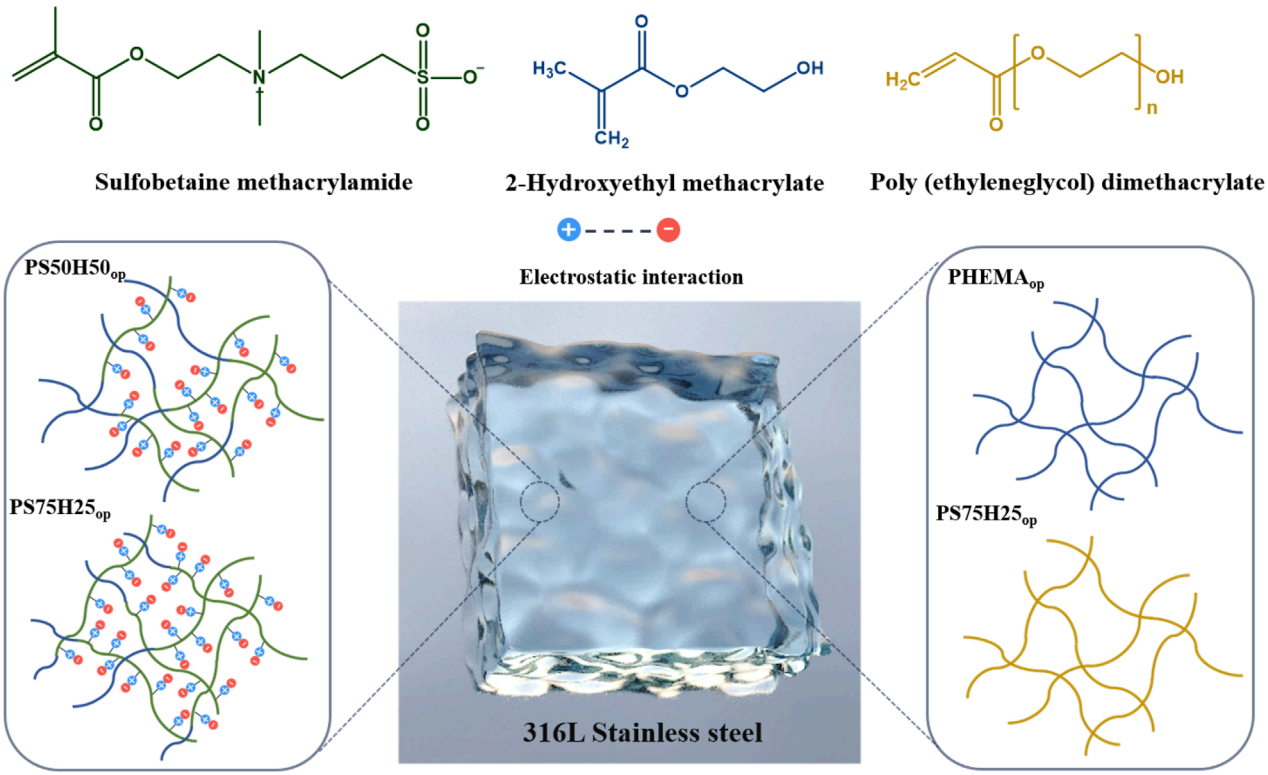

FIGURE 1
A schematic diagram of the hydrogels composed of different ratios of SBMA, HEMA and PEGMA segments.

and 602 cm^{-1} respectively belonged to the sulfonate groups (SO_3^-) and C-S stretching vibration, and the adsorption intensities of these vibrations increased as SBMA content (Tian et al., 2013; Wu et al., 2017). These results demonstrated the successful synthesis of various hydrogel coatings.

Mechanical stability of the hydrogel coatings

The excellent biocompatibility and drug-loading performance of hydrogels makes them a strong candidate for biomedical applications. However, the inadequate mechanical properties of hydrogels make the swollen hydrogel coatings easy to collapse and detach from the material surface during transport and service (Yao et al., 2022; Wei et al., 2023a; Wei et al., 2023b). In order to systematically assess the mechanical stability of the hydrogel coatings, we evaluated their weight loss after the immersion swelling, flow and tape-peeling tests (Figure 3). In the flow test, the flow rate was set to 500 mL min^{-1} to simulate the real blood flow rate in an artery (Obiweluozor et al., 2019). $PS50H50_{op}$ experienced almost no weight loss in swelling and tape-peeling tests (Figures 3A, C), while only ~3% weight loss was observed after the flow test (Figure 3B). Copolymerizing HEMA segments highly improved the mechanical stability of zwitterionic hydrogel coatings. Moghadam *et al.* highlighted the key role of the hydrophobicity of HEMA in increasing the mechanical properties of those fragile and mechanically poor hydrophilic hydrogels (Moghadam and Pioletti, 2015). The mechanical stability of the coatings deteriorated as the SBMA component increased. PS75H25op coatings experienced significant weight loss in the swelling test (~40%) and flow test (~60%). The inadequate addition of HEMA segments could not reverse the poor mechanical stability of SBMA hydrogel coatings. It is worth noting that, although the pure HEMA coatings exhibited good resistance to swelling and flow damages, they lost up to ~60% weight after tape-peeling tests. Due to the lack of toughness in $PHEMA_{op}$ hydrogel coatings, they were unable to form an effective cushion zone to resist deformation and dissipate energy in an abrasion environment, ultimately leading to the fracture of the polymer network (Moghadam and Pioletti, 2014). Similarly, ~80% weight loss was observed for pure $PEGMA_{op}$ hydrogel coatings after these three kinds of damage. The results indicated that it also remained a challenge to optimize the mechanical stability of pure HEMA or PEG hydrogel coatings solely by tailoring the various synthesis parameters. The adequate introduction of lubricative SBMA segments was crucial, which endowed an improved property of $PS50H50_{op}$ coatings to resist multiple damages, especially abrasion damage (Wei et al., 2013; Adibnia et al., 2020). On the basis of the results above, $PS50H50_{op}$ coatings showed the best mechanical stability among these four coatings, resulting from the good integration of SBMA and HEMA.

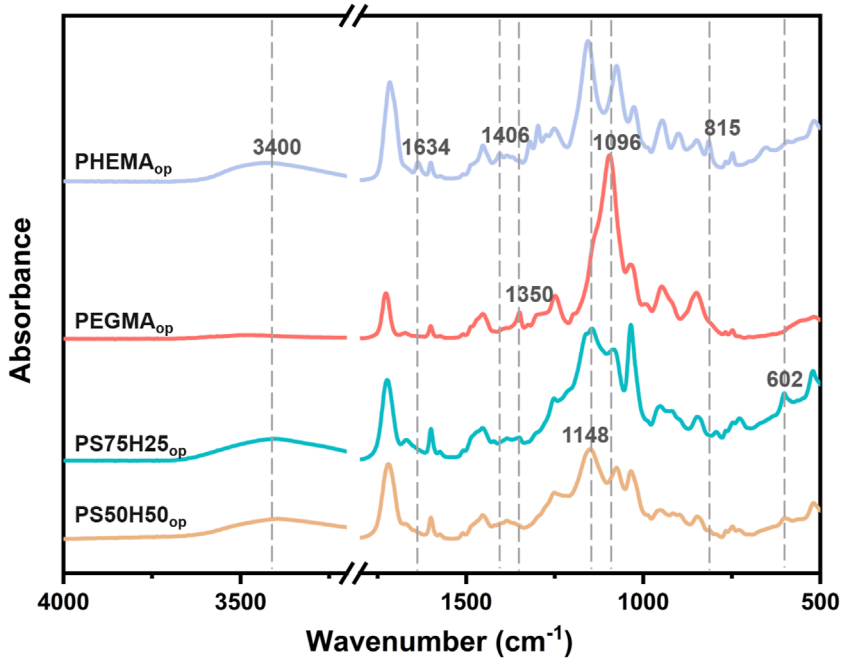

FIGURE 2
The FTIR spectra of the hydrogel coatings.

Drug release behaviors from hydrogel coatings

The swellability of hydrogel coatings may correlate positively with their drug-loading capacity (Tronci et al., 2014; Capanema et al., 2018). Therefore, the equilibrium water content (EWC) of different hydrogel coatings was first investigated. As shown in Figure 4, the water content of all hydrogel coatings increased sharply before 2 h and exhibited no significant change in the time interval of 2–8 h. Hydrogel coatings have been completely swollen within 2 h, and could no longer absorb more water from the external environment after reaching the equilibrium. The EWC (~69%) of PHEMA$_{op}$ was the lowest among these four hydrogel coatings. The introduction of 50% and 75% SBMA components increased the water content of the hydrogel coatings to ~487% and ~521% at the immersion time of 1 h, respectively. This phenomenon was mainly attributed to the hydrogen bonding and ionic solvation effect of SBMA that could accommodate more water molecules around the polymer network, significantly enhancing the swellability of hydrogel coatings (Li et al., 2022). As the immersion time increased, the water content of PS50H50$_{op}$ increased to ~676% and coatings reached the equilibrium. However, no equilibrium was observed for PS75H25$_{op}$ coatings, their water content decreased continuously during the immersion time of 2–8 h. These results could be explained by the weak stability of the PS75H25$_{op}$ coatings as revealed by the tests in Section 3.2. In addition, PEGMA$_{op}$ showed similar swellability to PS50H50$_{op}$, as their EWC also reached to ~682%.

Subsequently, UV-Vis measurements were performed to quantitatively determine the drug release behaviors of D-mix and gentamicin from hydrogel coatings. The UV-Vis spectra of the D-mix at different concentrations were shown in Figure 5A. The intensity of the absorption peak located at 278 nm was used to be linearly fitted to plot the standard curve (Figure 5B) and quantify the concentration of D-mix (Liu et al., 2017; Hao et al., 2021). As shown in Figure 5C, all four hydrogel coatings reached the drug release limit within 24 h, and released almost no D-mix into the water environment during the period of 24–48 h. The drug release amount from PS50H50$_{op}$ and PEGMA$_{op}$ coatings was the highest, releasing ~40 ppm D-mix at the immersion time of 24 h. These results were attributed to their excellent swellability (Figure 4), allowing more D-mix absorbed into the hydrogel network. Compared to PS50H50$_{op}$ coating, PS75H25$_{op}$ coatings integrated more SBMA segments but finally released fewer D-mix (~23 ppm). This was because of the breakage of the swollen PS75H25$_{op}$ hydrogel network during the immersion, leading to a significant decrease in the drug-loading capacity of hydrogels, which was evidenced by the ~40% hydrogels separated from the material surfaces after the immersion tests (Figure 3A). The PHEMA$_{op}$ hydrogel coatings only released ~8 ppm of D-mix within 24 h due to its poor swelling performance.

Due to the inability to detect the characteristic peak of gentamicin via UV-Vis spectra, the polycondensation between o-phthalaldehyde and gentamicin was employed and the characteristic UV-Vis peak intensities at 332 nm (Figure 6A) of products in isopropanol were detected to plot the standard curve (Figure 6B) and quantify the concentration of gentamicin (Figure 6C). Similarly, the PS50H50$_{op}$ and PEGMA$_{op}$ hydrogel coatings showed the highest release amount (~13 ppm) of gentamicin, while the PEGMA$_{op}$ and PHEMA$_{op}$ hydrogel coatings (~2.6 ppm)

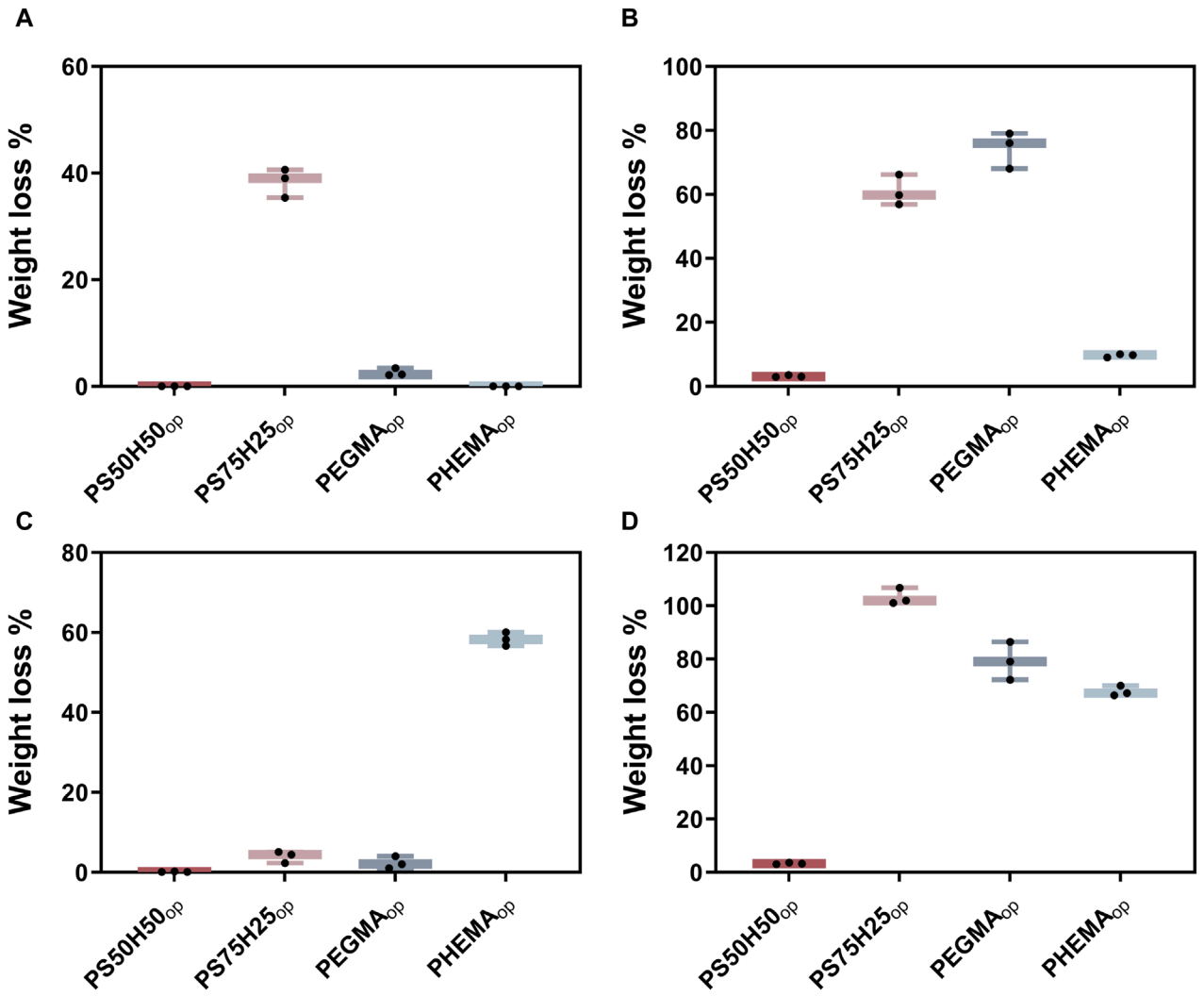

FIGURE 3
Mechanical stability of different hydrogel coatings. Weight loss of hydrogel coatings after **(A)** immersion swelling, **(B)** flow and **(C)** tape-peeling tests; **(D)** the total weight loss after these three tests.

released fewer drugs during the immersion time of 48 h, 7.8 ppm and ~2.6 ppm respectively. It is worth noting that, the release behaviors of gentamicin and D-mix were almost synchronous. During each time interval, the release amount of gentamicin from the hydrogel coatings was always ~1/3 of D-mix, which was consistent with the optimized ratio of gentamicin to D-mix in the drug combinations. These results provided the basics to achieve the optimal antibiofilm and antimicrobial of hydrogel coatings. Generally speaking, $PS50H50_{op}$ hydrogel coatings possessed a higher drug release concentration and a faster release speed than nanocapsules (Huang et al., 2017b; Wang et al., 2022), which prevented the bacteria from escaping the sub-inhibitory concentrations of antibiotics and transferring drug-resistant genes to their descendants. The above results highlighted the potential application of PS50H50op hydrogel coatings to completely inhibit the biofilms associated bacterial infections.

Antibiofilm and antimicrobial activities of hydrogel coatings

The antibiofilm activity of the D-mix, gentamicin and their combinations were first evaluated in terms of the biofilm formation inhibition via CV staining assay. As shown in Figure 7A, using D-mix alone exhibited marginal antibiofilm activity. Only ~20% biofilm formation was inhibited after the treatment of D-mix for 48 h. Benefiting from the bactericidal property, using gentamicin alone exhibited ~40% antibiofilm efficiency. However, D-mix/gentamicin combinations inhibited more than 90% biofilm formation, showing significantly higher antibiofilm efficiency than employing only a single mechanism. The potent antibiofilm activity of the combinations was attributed to the ability of D-mix to integrate into the peptidoglycan of bacterial cells and change multiple positions of the peptidoglycan-peptide bridge, resulting in maximum inhibition of *P. aeruginosa* biofilm formation. In the

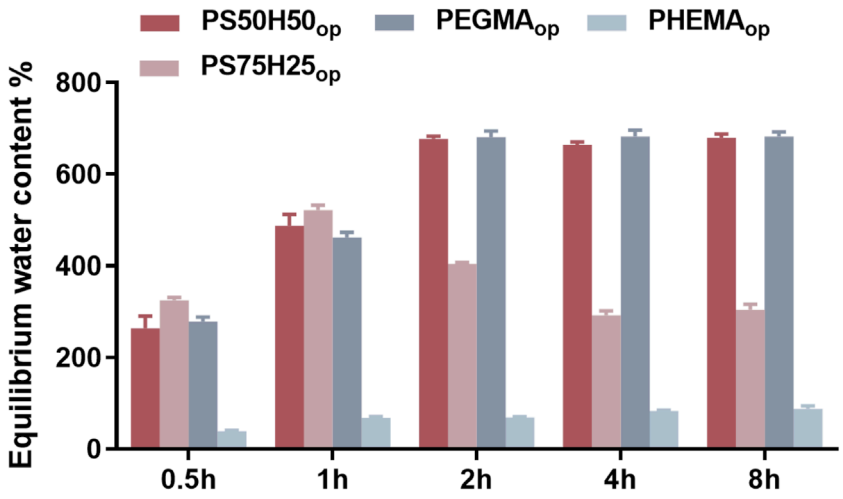

FIGURE 4
The equilibrium water content of the different hydrogel coatings.

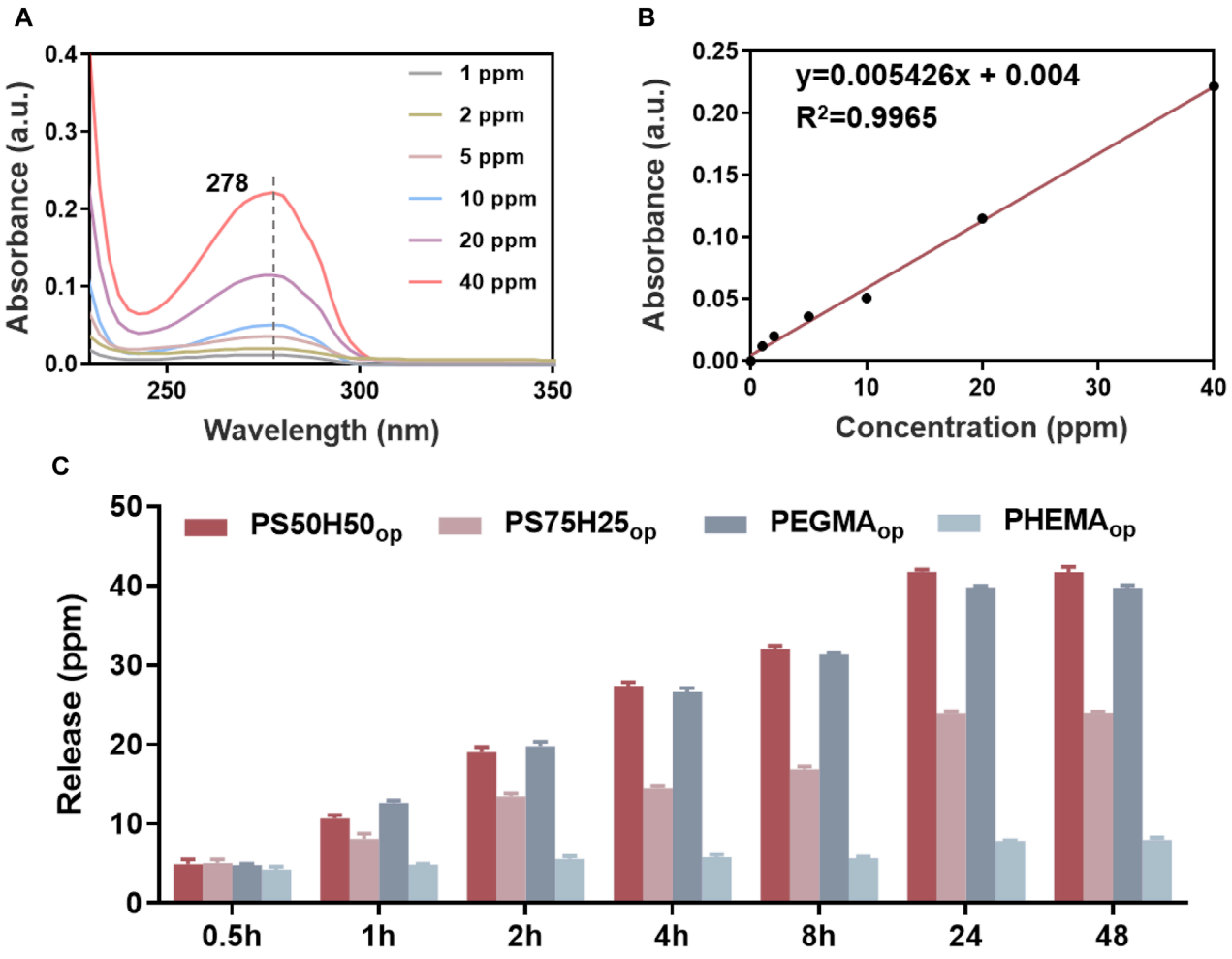

FIGURE 5
(A) Standard UV-Vis spectra of D-mix in deionized water; **(B)** the linear fitted curve between the characteristic peak intensities at 278 nm and the corresponding concentration of D-mix; **(C)** the release amount of D-mix from different hydrogel coatings.

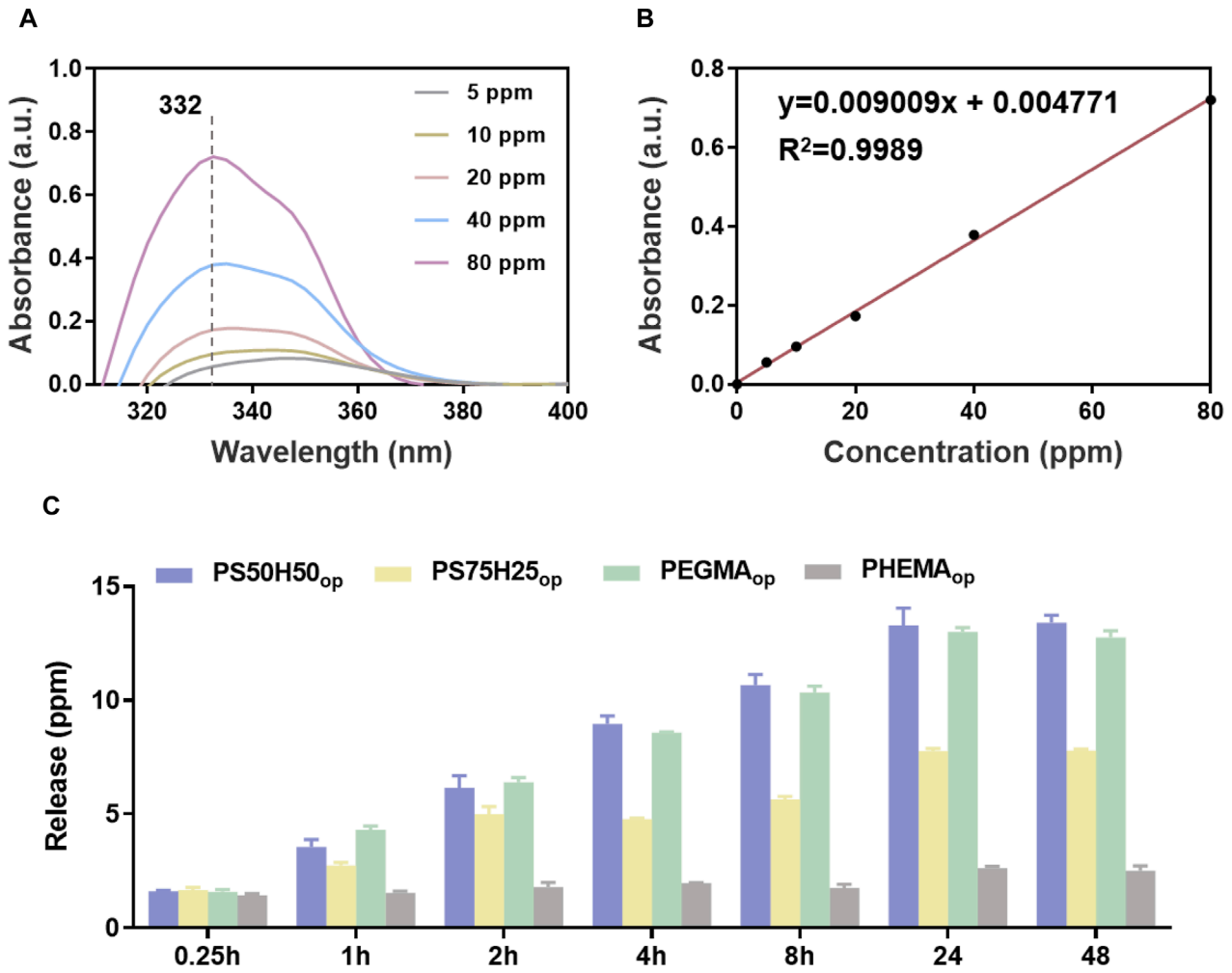

FIGURE 6
(A) Standard UV-Vis spectra of gentamicin in isopropanol; **(B)** the linear fitted curve between the characteristic peak intensities at 332 nm and the corresponding concentration of gentamicin; **(C)** the release amount of gentamicin from different hydrogel coatings.

absence of biofilm, bacteria were forced to survive in planktonic form, in which they were much more susceptive to the harm of gentamicin.

Subsequently, the spread plate method was employed to evaluate the antimicrobial activities of hydrogel coating surfaces (Jin et al., 2022). As shown in Figures 7B–D, $PS50H50_{op}$ and $PEGDA_{op}$ hydrogel coatings exhibited excellent antimicrobial activities, with the logarithmic inhibition rates of bacterial growth on the surfaces reaching 2.3 (>99.6%) and 2.0 (>98.9%), respectively. These antimicrobial activities were mainly attributed to the antifouling properties of the coatings themselves and the releases of D-mix/gentamicin combinations. Compared to $PS50H50_{op}$ coatings, the logarithmic antimicrobial efficiency of $PS75H25_{op}$ coatings was significantly reduced to 1.1. $PS75H25_{op}$ coatings partly separated from the substrate during the 24 h immersion due to the inadequate mechanical stability. The bare stainless steel surfaces could not resist the bacterial attachment. Among these four hydrogel coatings, the logarithmic antimicrobial efficiency of $PHEMA_{op}$ coatings was only 0.9. Although $PHEMA_{op}$ coatings exhibited excellent mechanical stability during the immersion, the inadequate drug-loading capacity of them (Figures 5, 6) was a key reason for their lowest antimicrobial activities. The CLSM method was used to further evaluate the bacterial colonization on the hydrogel coating surfaces (Figure 8). *P. aeruginosa* was visualized under a microscope after staining with SYTO-9 and PI dyes. SYTO-9 dyes could penetrate the bacterial cell membranes to label the DNA (or RNA) of both live and dead bacteria with green fluorescence. In contrast, PI dyes only penetrated damaged cell membranes to identify dead bacteria with red fluorescence. On the surface of bare steel, living *P. aeruginosa* were densely distributed under biofilms. Bacterial infections associated with biofilms were extremely difficult to eliminate even via surgical means because residual bacteria would result in recurrent infections for patients (Gao et al., 2020). Almost no bacteria were visible on the surface of $PS50H50_{op}$ coatings. The D-mix/gentamicin combinations released from the hydrogels rapidly killed the live bacteria and inhibited residual bacteria from forming biofilms. Moreover, the dense water film produced by SBMA segments further prevented the attachment of dead bacteria.

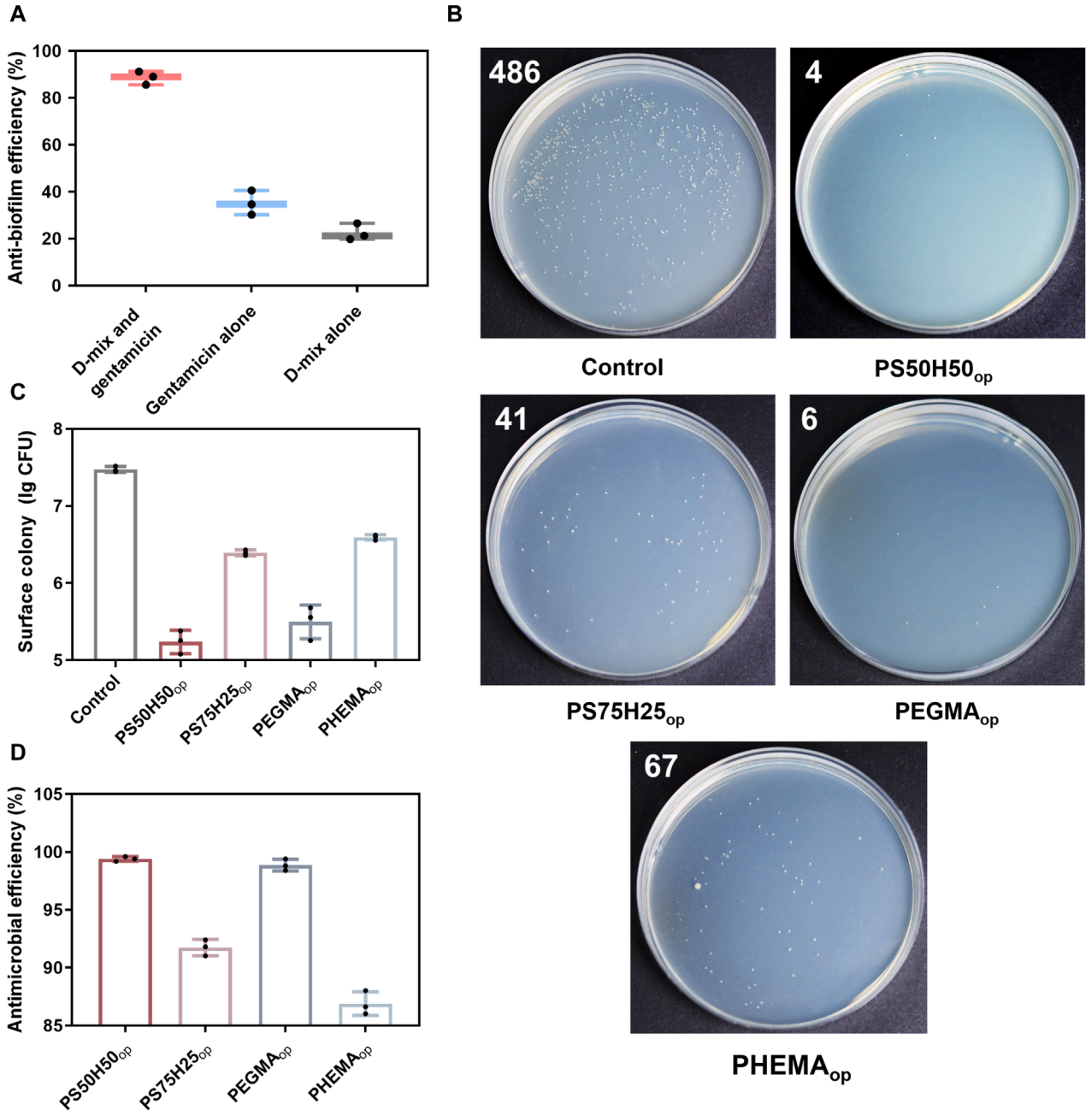

FIGURE 7
(A) Antibiofilm efficiency of D-mix, gentamicin alone and their drug combinations calculated by the CV staining assay; **(B)** Digital images of LB agar plates (the white number represents the quantity of the visible colonies on the plates) and **(C)** corresponding statistical data of *P. aeruginosa* on the surface treated with different hydrogels; **(D)** Antimicrobial efficiency of hydrogel coatings calculated by the number of surface colony.

In contrast, some dead bacteria could be seen attached to the surfaces of $PS75H25_{op}$ and $PHMEA_{op}$ coatings. The accumulation of dead bacteria may also hide the function of coatings, leading to their failure in long-term applications (Hartleb et al., 2015). Moreover, the mechanical stability of the coatings was a highly concerning issue for their long-term applications. Yuan *et al.* claimed the significance of mechanical stability of medical implant coatings and designed a stable antimicrobial peptide coating through a layer-by-layer self-assembly method. The covered implants were able to reduce bacterial colonization by up to 3.2 log even after repeated usage (Yuan et al., 2019). Therefore, the antimicrobial efficiency of $PS50H50_{op}$ coatings was also assessed after being subjected to swelling, flushing and abrasion damages. As shown in Figure 9, the fluorescence intensities on treated $PS50H50_{op}$ coatings were similar to the original ones, demonstrating that $PS50H50_{op}$ coatings remained the excellent antimicrobial activities

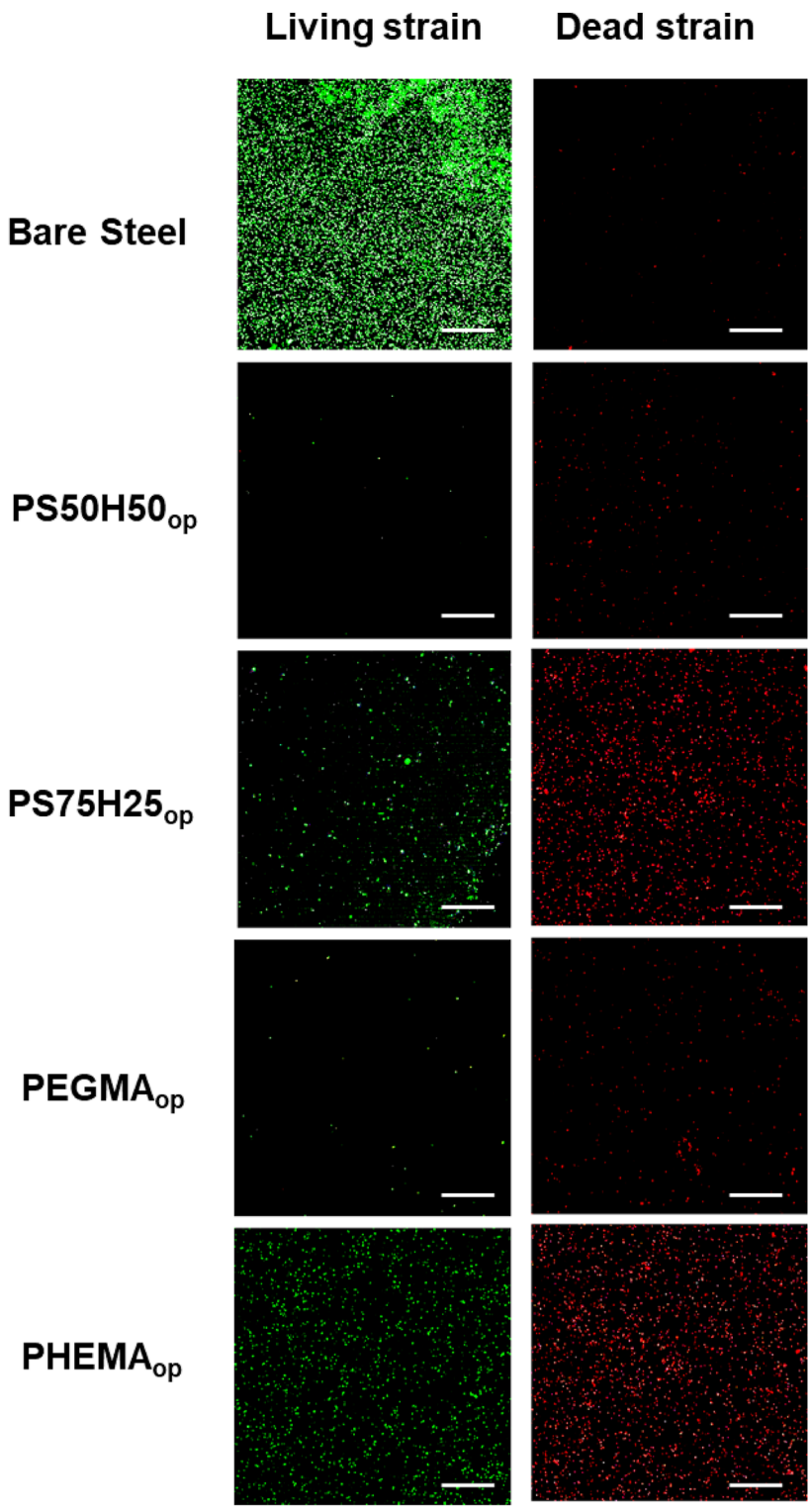

FIGURE 8
Typical CLSM of *P. aeruginosa* on the surface treated with different hydrogels after 24 h of incubation. The scale bar represents 100 μM.

after multiple damages. Moreover, the bacteria on the surfaces of $PS50H50_{op}$ coatings did not further proliferate after 72 h of immersion. The results further confirmed the excellent mechanical stability of $PS50H50_{op}$ hydrogel coatings.

Conclusion

In summary, a D-mix/gentamicin loaded SBMA-HEMA hydrogel coating with optimized mechanical stability and biofilm

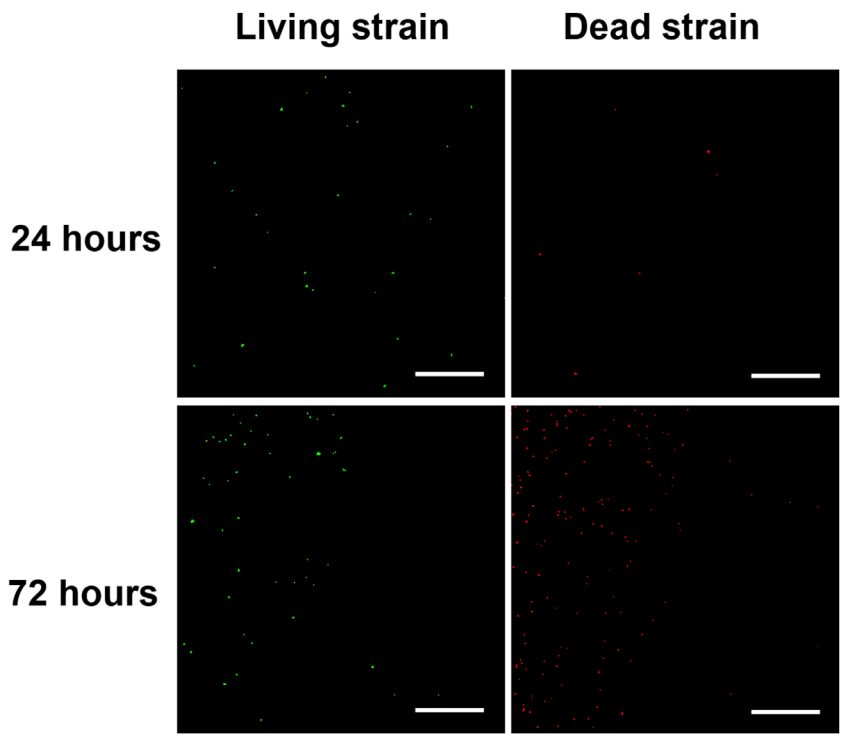

FIGURE 9
Typical CLSM of *P. aeruginosa* on the treated PS50H50$_{op}$ coating surfaces after 24 and 72 h incubation. The scale bar represents 100 μM.

inhibition capabilities was prepared on the 316 L stainless steel surface. The weight loss tests indicated that the adequate integration of HEMA with SBMA segments significantly enhanced the stability of hydrogel coatings against mechanical damages. The weight of PS50H50$_{op}$ coatings was well retained after subjected swelling, flushing and abrasion damages. The obtained PS50H50$_{op}$ coatings were able to effectively inhibit the growth of *P. aeruginosa* and the biofilm formation. This was done with the synergy of the D-mix and gentamicin loaded in the hydrogel coatings. The D-mix exerted a stronger biofilm formation inhibition and maintained bacteria in the planktonic state, facilitating the bactericidal action of gentamicin. Owing to the strong mechanical stability, the excellent antibiofilm and antimicrobial activities of PS50H50$_{op}$ coatings were well preserved after multiple mechanical damages. The fine-designed PS50H50$_{op}$ hydrogel coatings provide an effective method to treat biofilms associated bacterial infections on the material surfaces.

Data availability statement

The original contributions presented in the study are included in the article/supplementary material, further inquiries can be directed to the corresponding author.

Author contributions

JY: Investigation, Methodology, Writing–original draft. YR: Investigation, Methodology, Writing–original draft. JZ: Methodology, Writing–original draft. TX: Investigation, Writing–original draft. XH: Investigation, Writing–review and editing. DZ: Conceptualization, Supervision, Writing–review and editing.

Funding

The author(s) declare financial support was received for the research, authorship, and/or publication of this article. The work was supported by Beijing Nova Program (20220484224) and Interdisciplinary Research Project for Young Teachers of USTB (FRF-IDRY-21-021).

Conflict of interest

The authors declare that the research was conducted in the absence of any commercial or financial relationships that could be construed as a potential conflict of interest.

Publisher's note

References

Adibnia, V., Olszewski, M., De-Crescenzo, G., Matyjaszewski, K., and Banquy, X. (2020). Superlubricity of zwitterionic bottlebrush polymers in the presence of multivalent ions. *J. Am. Chem. Soc.* 142, 14843–14847. doi:10.1021/jacs.0c07215

Bjarnsholt, T., Alhede, M., Alhede, M., Eickhardt-Sorensen, S. R., Moser, C., Kuhl, M., et al. (2013). The *in vivo* biofilm. *Trends. Microbiol.* 21, 466–474. doi:10.1016/j.tim.2013.06.002

Brauner, A., Fridman, O., Gefen, O., and Balaban, N. Q. (2016). Distinguishing between resistance, tolerance and persistence to antibiotic treatment. *Nat. Rev. Microbiol.* 14, 320–330. doi:10.1038/nrmicro.2016.34

Busscher, H., Mei, H. C., Subbiahdoss, G., Jutte, P. C., Dungen, J. J. A. M., Zaat, S. A. J., et al. (2012). Biomaterial-associated infection: locating the finish line in the race for the surface. *Sci. Transl. Med.* 4, 153rv110. doi:10.1126/scitranslmed.3004528

Cao, B., Lee, C. J., Zeng, Z., Cheng, F., Xu, F., Cong, H., et al. (2016). Electroactive poly(sulfobetaine-3,4-ethylenedioxythiophene) (PSBEDOT) with controllable antifouling and antimicrobial properties. *Chem. Sci.* 7, 1976–1981. doi:10.1039/c5sc03887a

Capanema, N., Mansur, A., Jesus, A., Carvalho, S., Oliveira, L., and Mansur, H. (2018). Superabsorbent crosslinked carboxymethyl cellulose-PEG hydrogels for potential wound dressing applications. *Int. J. Biol. Macromol.* 106, 1218–1234. doi:10.1016/j.ijbiomac.2017.08.124

Caparros, M., Pisabarro, A., and Pedro, M. A. (1992). Effect of D-amino acids on structure and synthesis of peptidoglycan in *Escherichia coli*. *J. Bacteriol.* 174, 5549–5559. doi:10.1128/jb.174.17.5549-5559.1992

Conrad, R. S., Massey, L. K., and Sokatch, J. R. (1974). D-and L-isoleucine metabolism and regulation of their pathways in Pseudomonas putida. *J. Bacteriol.* 118, 103–111. doi:10.1128/jb.118.1.103-111.1974

Dizon, G. V., Chou, Y. N., Yeh, L. C., Venault, A., Huang, J., and Chang, Y. (2018). Bio-inert interfaces via biomimetic anchoring of a zwitterionic copolymer on versatile substrates. *J. Colloid. Interface. Sci.* 529, 77–89. doi:10.1016/j.jcis.2018.05.073

Dulong, V., Lack, S., Cerf, D. L., Picton, L., Vannier, J. P., and Muller, G. (2004). Hyaluronan-based hydrogels particles prepared by crosslinking with trisodium trimetaphosphate. Synthesis and characterization. *Carbohydr. Polym.* 57, 1–6. doi:10.1016/j.carbpol.2003.12.006

Feng, T., Ji, W., Zhang, Y., Wu, F., Tang, Q., Wei, H., et al. (2020). Zwitterionic polydopamine engineered interface for *in vivo* sensing with high biocompatibility. *Angew. Chem. Int. Ed.* 59, 23445–23449. doi:10.1002/anie.202010675

Flemming, H., Wingender, J., Szewzyk, U., Steinberg, P. D., Rice, S. A., and Kjelleberg, S. (2016). Biofilms: an emergent form of bacterial life. *Nat. Rev. Microbiol.* 14, 563–575. doi:10.1038/nrmicro.2016.94

Gao, Q., Li, X., Yu, W., Jia, F., Yao, T., Jin, Q., et al. (2020). Fabrication of mixed-charge polypeptide coating for enhanced hemocompatibility and anti-infective effect. *ACS Appl. Mater. Interfaces* 12, 2999–3010. doi:10.1021/acsami.9b19335

Gong, Y. K., Liu, L. P., and Messersmith, P. B. (2012). Doubly biomimetic catecholic phosphorylcholine copolymer: a platform strategy for fabricating antifouling surfaces. *Macromol. Biosci.* 12, 979–985. doi:10.1002/mabi.201200074

Hao, X., Yang, J., Zhang, L., Ren, C., Li, W., Lou, Y., et al. (2021). pH-responsive d-leucine functional multilayer films with antibacterial and anti-adhesion synergistic properties. *Mater. Today Commun.* 28, 102691. doi:10.1016/j.mtcomm.2021.102691

Hartleb, W., Saar, J., Zou, P., and Lienkamp, K. (2015). Just antimicrobial is not enough: toward bifunctional polymer surfaces with dual antimicrobial and protein-repellent functionality. *Macromol. Chem. Phys.* 217, 225–231. doi:10.1002/macp.201500266

Hochbaum, A., Kolodkin-Gal, I., Foulston, L., Kolter, R., Aizenberg, J., and Losick, R. (2011). Inhibitory effects of D-amino acids on *Staphylococcus aureus* biofilm development. *J. Bacteriol.* 193, 5616–5622. doi:10.1128/JB.05534-11

Huang, D., Wang, J., Ren, K., and Ji, J. (2020a). Functionalized biomaterials to combat biofilms. *Biomater. Sci.* 8, 4052–4066. doi:10.1039/D0BM00526F

Huang, L., Lou, Y., Zhang, D., Ma, L., Qian, H., Hu, Y., et al. (2020b). d-Cysteine functionalised silver nanoparticles surface with a "disperse-then-kill" antibacterial synergy. *Chem. Eng. J.* 381, 122662. doi:10.1016/j.cej.2019.122662

Huang, T., Liu, H., Liu, P., Liu, P., Li, L., and Shen, J. (2017a). Zwitterionic copolymers bearing phosphonate or phosphonic motifs as novel metal-anchorable anti-fouling coatings. *J. Mater. Chem. B* 5, 5380–5389. doi:10.1039/c7tb01017f

Huang, Y., Liu, T., Ma, L., Wang, J., Zhang, D., and Li, X. (2017b). Saline-responsive triple-action self-healing coating for intelligent corrosion control. *Mater. Des.* 214, 110381. doi:10.1016/j.matdes.2022.110381

Jin, Z., Liu, H., Wang, Z., Zhang, W., Chen, Y., Zhao, T., et al. (2022). Enhancement of anticorrosion and antibiofouling performance of self-healing epoxy coating using nano-hydrotalcite materials and bifunctional biocide sodium pyrithione. *Prog. Org. Coat.* 172, 107121. doi:10.1016/j.porgcoat.2022.107121

Karatan, E., and Watnick, P. (2009). Signals, regulatory networks, and materials that build and break bacterial biofilms. *Microbiol. Mol. Biol. Rev.* 73, 310–347. doi:10.1128/MMBR.00041-08

Kardela, J. H., Millichamp, I. S., Ferguson, J., Parry, A. L., Reynolds, K., Aldred, N., et al. (2019). Nonfreezable water and polymer swelling control the marine antifouling performance of polymers with limited hydrophilic content. *ACS Appl. Mater. Interfaces* 11, 29477–29489. doi:10.1021/acsami.9b05893

Kim, S., English, A., and Kihm, K. (2009). Surface elasticity and charge concentration-dependent endothelial cell attachment to copolymer polyelectrolyte hydrogel. *Acta. Biomater.* 5, 144–151. doi:10.1016/j.actbio.2008.07.033

Kim, S. H., Kim, S. H., Nair, S., and Moore, E. (2005). Reactive electrospinning of cross-linked poly (2-hydroxyethyl methacrylate) nanofibers and elastic properties of individual hydrogel nanofibers in aqueous solutions. *Macromolecules* 38, 3719–3723. doi:10.1021/ma050308g

Kolodkin-Gal, I., Romero, D., Cao, S., Clardy, J., Kolter, R., and Losick, R. (2010). D-amino acids trigger biofilm disassembly. *Science.* 328, 627–629. doi:10.1126/science.1188628

Koo, H., Allan, R., Howlin, R., Stoodley, P., and Hall-Stoodley, L. (2017). Targeting microbial biofilms: current and prospective therapeutic strategies. *Nat. Rev. Microbiol.* 15, 740–755. doi:10.1038/nrmicro.2017.99

Li, B., Xie, J., Yuan, Z., Jain, P., Lin, X., Wu, K., et al. (2018). Mitigation of inflammatory immune responses with hydrophilic nanoparticles. *Angew. Chem. Int. Ed.* 57, 4527–4531. doi:10.1002/anie.201710068

Li, Q., Wen, C., Yang, J., Zhou, X., Zhu, Y., Zheng, J., et al. (2022). Zwitterionic biomaterials. *Chem. Rev.* 122, 17073–17154. doi:10.1021/acs.chemrev.2c00344

Lin, H., Wagner, E., Swinnea, J., Freeman, B., Pas, S., Hill, A., et al. (2006). Transport and structural characteristics of crosslinked poly(ethylene oxide) rubbers. *J. Membr. Sci.* 276, 145–161. doi:10.1016/j.memsci.2005.09.040

Liu, Z., Yang, J., Zhu, W., Zhou, S., and Tan, X. (2017). Measurement analysis of two radials with a common-origin point and its application. *Luminescence* 32, 800–805. doi:10.1002/bio.3254

Lopez, D., Vlamakis, H., and Kolter, R. (2009). Generation of multiple cell types in Bacillus subtilis. *FEMS Microbiol. Rev.* 33, 152–163. doi:10.1111/j.1574-6976.2008.00148.x

Moghadam, M., and Pioletti, D. (2015). Improving hydrogels' toughness by increasing the dissipative properties of their network. *J. Mech. Behav. Biomed. Mater.* 41, 161–167. doi:10.1016/j.jmbbm.2014.10.010

Moghadam, M., Pioletti, D., Vogel, A., and Klok, H. A. (2014). Controlled release from a mechanically-stimulated thermosensitive self-heating composite hydrogel. *Biomaterials* 35, 450–455. doi:10.1016/j.biomaterials.2013.09.065

Obiweluozor, F., Tiwari, A., Lee, J., Batgerel, T., Kim, J., Lee, D., et al. (2019). Thromboresistant semi-IPN hydrogel coating: towards improvement of the hemocompatibility/biocompatibility of metallic stent implants. *Mater. Sci. Eng. C* 99, 1274–1288. doi:10.1016/j.msec.2019.02.054

Pacaphol, K., and Aht-Ong, D. (2017). The influences of silanes on interfacial adhesion and surface properties of nanocellulose film coating on glass and aluminum substrates. *Surf. Coat. Techno.l.* 320, 70–81. doi:10.1016/j.surfcoat.2017.01.111

Pedro, M. A., Young, K. D., Holtje, J. V., and Schwarz, H. (2003). Branching of *Escherichia coli* cells arises from multiple sites of inert peptidoglycan. *J. Bacteriol.* 185, 1147–1152. doi:10.1128/JB.185.4.1147-1152.2003

Qian, H., Yang, J., Lou, Y., Rahman, O., Li, Z., Ding, X., et al. (2019). Mussel-inspired superhydrophilic surface with enhanced antimicrobial properties under immersed and atmospheric conditions. *Appl. Surf. Sci.* 465, 267–278. doi:10.1016/j.msec.2017.07.002

Sampath, S., and Robinson, D. (1990). Comparison of new and existing spectrophotometric methods for the analysis of tobramycin and other aminoglycosides. *J. Pharm. Sci.* 79, 428–431. doi:10.1002/jps.2600790514

Sanchez, C. J., Akers, K. S., Romano, D. R., Woodbury, R. L., Hardy, S. K., Murray, C. K., et al. (2014). D-amino acids enhance the activity of antimicrobials against biofilms of clinical wound isolates of *Staphylococcus aureus* and *Pseudomonas aeruginosa*. *Antimicrob. Agents. Chemother.* 58, 4353–4361. doi:10.1128/AAC.02468-14

She, P., Chen, L., Liu, H., Zou, Y., Luo, Z., Koronfel, A., et al. (2015). The effects of D-Tyrosine combined with amikacin on the biofilms of *Pseudomonas aeruginosa*. *Microb. Pathog.* 86, 38–44. doi:10.1016/j.micpath.2015.07.009

Sin, M. C., Chen, S. H., and Chang, Y. (2014). Hemocompatibility of zwitterionic interfaces and membranes. *Polym. J.* 46, 436–443. doi:10.1038/pj.2014.46

Tan, G., Wang, Y., Li, J., and Zhang, S. (2008). Synthesis and characterization of injectable photocrosslinking poly (ethylene glycol) diacrylate based hydrogels. *Polym. Bull.* 61, 91–98. doi:10.1007/s00289-008-0932-8

Tian, M., Wang, J., Zhang, E., Li, J., Duan, C., and Yao, F. (2013). Synthesis of agarose-graft-poly[3-dimethyl (methacryloyloxyethyl) ammonium

propanesulfonate] zwitterionic graft copolymers via ATRP and their thermally-induced aggregation behavior in aqueous media. *Langmuir* 29, 8076–8085. doi:10.1021/la4007668

Tong, Z., Zhang, L., Ling, J., Jian, Y., Huang, L., and Deng, D. (2014). An *in vitro* study on the effect of free amino acids alone or in combination with nisin on biofilms as well as on planktonic bacteria of Streptococcus mutans. *PLoS One* 9, e99513. doi:10.1371/journal.pone.0099513

Tronci, G., Ajiro, H., Russell, S., Wood, D., and Akashi, M. (2014). Tunable drug-loading capability of chitosan hydrogels with varied network architectures. *Acta. Biomater.* 10, 821–830. doi:10.1016/j.actbio.2013.10.014

Wang, J., Ma, L., Guo, X., Wu, S., Liu, T., Yang, J., et al. (2022). Two birds with one stone: nanocontainers with synergetic inhibition and corrosion sensing abilities towards intelligent self-healing and self-reporting coating. *Chem. Eng. J.* 433, 134515. doi:10.1016/j.cej.2022.134515

Warraich, A., Mohammed, A., Perrie, Y., Hussain, M., Gibson, H., and Rahman, A. (2020). Evaluation of anti-biofilm activity of acidic amino acids and synergy with ciprofloxacin on *Staphylococcus aureus* biofilms. *Sci. Rep.* 10, 9021. doi:10.1038/s41598-020-66082-x

Wegst, U. G. K., Bai, H., Saiz, E., Tomsia, A., and Ritchie, R. (2015). Bioinspired structural materials. *Nat. Mater.* 14, 23–36. doi:10.1038/nmat4089

Wei, Q., Cai, M., Zhou, F., and Liu, W. (2013). Dramatically tuning friction using responsive polyelectrolyte brushes. *Macromolecules* 46, 9368–9379. doi:10.1021/ma401537j

Wei, Y., Cao, X., Hu, J., Li, N., Sun, L., Li, W., et al. (2023b). Preparation of salt-tolerant chitosan hydrogels and their anti-biofouling behavior study. *Surf. Coat. Tech.* 460, 129403. doi:10.1016/j.surfcoat.2023.129403

Wei, Y., Li, W., Liu, H., and Liu, H. (2023a). *In situ* preparation of spindle calcium carbonate-chitosan/poly (vinylalcohol) anti-biofouling hydrogels inspired by shellfish. *J. Ind. Eng. Chem.* 121, 499–509. doi:10.1016/j.jiec.2023.02.005

Wu, J., He, C., He, H., Cheng, C., Zhu, J., Xiao, Z., et al. (2017). Importance of zwitterionic incorporation into polymethacrylate-based hydrogels for simultaneously improving optical transparency, oxygen permeability, and antifouling properties. *J. Mater. Chem. B* 5, 4595–4606. doi:10.1039/c7tb00757d

Xing, J., Deng, L., Xie, C., Xiao, L., Zhai, Y., Jin, F., et al. (2011). Methoxy poly(ethylene glycol)-*b*-poly(octadecanoic anhydride)-*b*-methoxy poly(ethylene glycol) amphiphilic triblock copolymer nanoparticles as delivery vehicles for paclitaxel. *Adv. Technol.* 22, 669–674. doi:10.1002/pat.1563

Xu, H., and Liu, Y. (2011). Reduced microbial attachment by D-amino acid-inhibited AI-2 and EPS production. *Water. Res.* 45, 5796–5804. doi:10.1016/j.watres.2011.08.061

Yang, J., Qian, H., Wang, J., Ju, P., Lou, Y., Li, G., et al. (2021). Mechanically durable antibacterial nanocoatings based on zwitterionic copolymers containing dopamine segments. *J. Mater. Sci. Technol.* 89, 233–241. doi:10.1016/j.jmst.2020.11.031

Yang, J., Ran, Y., Huang, L., Ren, C., Hao, X., Ma, L., et al. (2023a). High-throughput screening of zwitterion-based coatings towards improved mechanical stability and drug-loading capacity. *npj Mater. Degrad.* 7, 51. doi:10.1038/s41529-023-00362-5

Yang, J., Ran, Y., Liu, S., Ren, C., Lou, Y., Ju, P., et al. (2023b). Synergistic D-Amino acids based antimicrobial cocktails formulated via high-throughput screening and machine learning. *Adv. Sci.* 11, e2307173. doi:10.1002/advs.202307173

Yao, M., Wei, Z., Li, J., Guo, Z., Yan, Z., Sun, X., et al. (2022). Microgel reinforced zwitterionic hydrogel coating for blood-contacting biomedical devices. *Nat. Commun.* 13, 5339. doi:10.1038/s41467-022-33081-7

Yuan, P., Qiu, X., Wang, X., Tian, R., Wang, L., Bai, Y., et al. (2019). Substrate-independent coating with persistent and stable antifouling and antibacterial activities to reduce bacterial infection for various implants. *Adv. Healthc. Mater.* 8, e1801423. doi:10.1002/adhm.201801423

Zeng, R., Cheng, J., Xu, S., Liu, Q., Wen, X., and Pi, P. (2014). Synthesis and drug-release studies of low-fouling zwitterionic hydrogels with enhanced mechanical strength. *J. Appl. Polym. Sci.* 131, 41041. doi:10.1002/app.41041